

NOT DEAD YET: COOL CIRCUMGALACTIC GAS IN THE HALOS OF EARLY TYPE GALAXIES¹

CHRISTOPHER THOM², JASON TUMLINSON², JESSICA K. WERK³, J. XAVIER PROCHASKA³, BENJAMIN D. OPPENHEIMER⁴, MOLLY S. PEEPLES⁵, TODD M. TRIPP⁶, NEAL S. KATZ⁶, JOHN M. O'MEARA⁷, AMANDA BRADY FORD⁸, ROMEEL DAVÉ⁸, KENNETH R. SEMBACH², DAVID H. WEINBERG⁹

Draft version October 29, 2018

ABSTRACT

We report new observations of circumgalactic gas in the halos of early type galaxies obtained by the COS-Halos Survey with the Cosmic Origins Spectrograph onboard the Hubble Space Telescope. We find that detections of H I surrounding early type galaxies are typically as common and strong as around star-forming galaxies, implying that the total mass of circumgalactic material is comparable in the two populations. For early type galaxies, the covering fraction for H I absorption above 10^{16} cm^{-2} is $\sim 40\text{--}50\%$ within ~ 150 kpc. Line widths and kinematics of the detected material show it to be cold ($T \lesssim 10^5$ K) in comparison to the virial temperature of the host halos. The implied masses of cool, photoionized CGM baryons may be up to $10^9 - 10^{11} M_{\odot}$. Contrary to some theoretical expectations, strong halo H I absorbers do not disappear as part of the quenching of star-formation. Even passive galaxies retain significant reservoirs of halo baryons which could replenish the interstellar gas reservoir and eventually form stars. This halo gas may feed the diffuse and molecular gas that is frequently observed inside ETGs.

Subject headings: galaxies: halos — galaxies: formation — quasars: absorption lines — intergalactic medium

1. GAS AND QUENCHING IN EARLY TYPE GALAXIES

The dichotomy of color, star-formation rate, morphology, etc. between spirals and early-type galaxies (ETGs) was established nearly a century ago, and has been highly refined over the past decade (e.g. Baldry et al. 2004; Bell et al. 2004; Faber et al. 2007). Despite long-standing empirical measurements, the physical processes that divide the two populations are still uncertain. The main challenge is to identify the mechanism(s) that quench star-formation (SF) and that inhibited it over the past ~ 10 Gyr. Dramatically different scenarios have been proposed for how star formation is quenched. Ejective feedback is generally caused by the galaxy itself, and includes super winds that expel gas (e.g. Springel et al. 2005) or more general heating and stripping of the gas (Tonnesen & Bryan 2009), as well as mergers. Conversely, preventative feedback, such as shock-heating of the gas prior to its accretion (e.g. Dekel & Birnboim 2006) or the disruption of in-falling clouds and their diffusion into the galaxy's gaseous halo (Putman et al. 2011;

Bland-Hawthorn et al. 2007), are consequences of ETGs living in massive halos.

The paradigm of 'red and dead' galaxies as quiescent, passively evolving stellar systems is being reconsidered in light of findings that a non-negligible fraction of them contain gas and dust, and a subset have experienced recent SF (e.g. Lees et al. 1991; González 1993; Trager et al. 2000; Thomas et al. 2010; Kaviraj 2010). There is also a high incidence of field ETGs with molecular gas (22%, Young et al. 2011), H I gas (40%, Serra et al. 2011), and ionized gas (73%, Davis et al. 2011). The gas masses are often comparable to those of spirals in both atomic and molecular phases, with $M_{\text{HI}} \sim 1 - 50 \times 10^7 M_{\odot}$ (Oosterloo et al. 2010) and $M_{\text{H}_2} = 10^{7-9} M_{\odot}$ (Figure 6 of Young et al. 2011). The corresponding SFRs reach up to a few $M_{\odot} \text{ yr}^{-1}$ (Crocker et al. 2011). Nevertheless, most ETGs are quenched, and remain so. These observations raise a new series of challenges: What is the source of the interstellar gas? On what time scale(s) did it arrive? Given this reservoir of cool gas, why does the SFR remain low?

2. THE COS-HALOS SURVEY: MOTIVATIONS AND DATA

Gas entering ETGs from their large-scale surroundings must pass through their circumgalactic medium (CGM), where it is detectable with sensitive UV absorption-line tracers (limiting column density $N_{\text{HI}} \gtrsim 10^{13} \text{ cm}^{-2}$). Quasar absorption line studies have attempted to link H I absorption (generally Ly α only) and nearby galaxies, but the results have been inconclusive, suffering from small sample sizes and the inability to control for galaxy type and SFR. Chen et al. (2001) showed that Ly α absorption is common around galaxies of a wide range of morphological types, whereas Chen & Mulchaey (2009) showed that strong H I absorbers ($N_{\text{HI}} > 10^{14} \text{ cm}^{-2}$) do not correlate with ETGs (see their Figure 13). Wakker & Savage (2009) found ubiquitous H I around $\gtrsim 0.1 L^*$ galaxies at 350 kpc scales, but could not separate galaxies by type.

¹ Based on observations made with the NASA/ESA Hubble Space Telescope, obtained at the Space Telescope Science Institute, which is operated by the Association of Universities for Research in Astronomy, Inc., under NASA contract NAS 5-26555. These observations are associated with program GO11598.

² Space Telescope Science Institute, 3700 San Martin Drive, Baltimore, MD, 21218, USA

³ UCO/Lick Observatory, University of California, Santa Cruz, CA

⁴ Leiden Observatory, Leiden University, the Netherlands

⁵ Center for Galaxy Evolution Fellow, University of California Los Angeles, Los Angeles, CA

⁶ Department of Astronomy, University of Massachusetts, Amherst, MA

⁷ Department of Chemistry and Physics, Saint Michael's College, Colchester, VT

⁸ Steward Observatory, University of Arizona, Tucson, AZ

⁹ Department of Astronomy, The Ohio State University, Columbus, OH

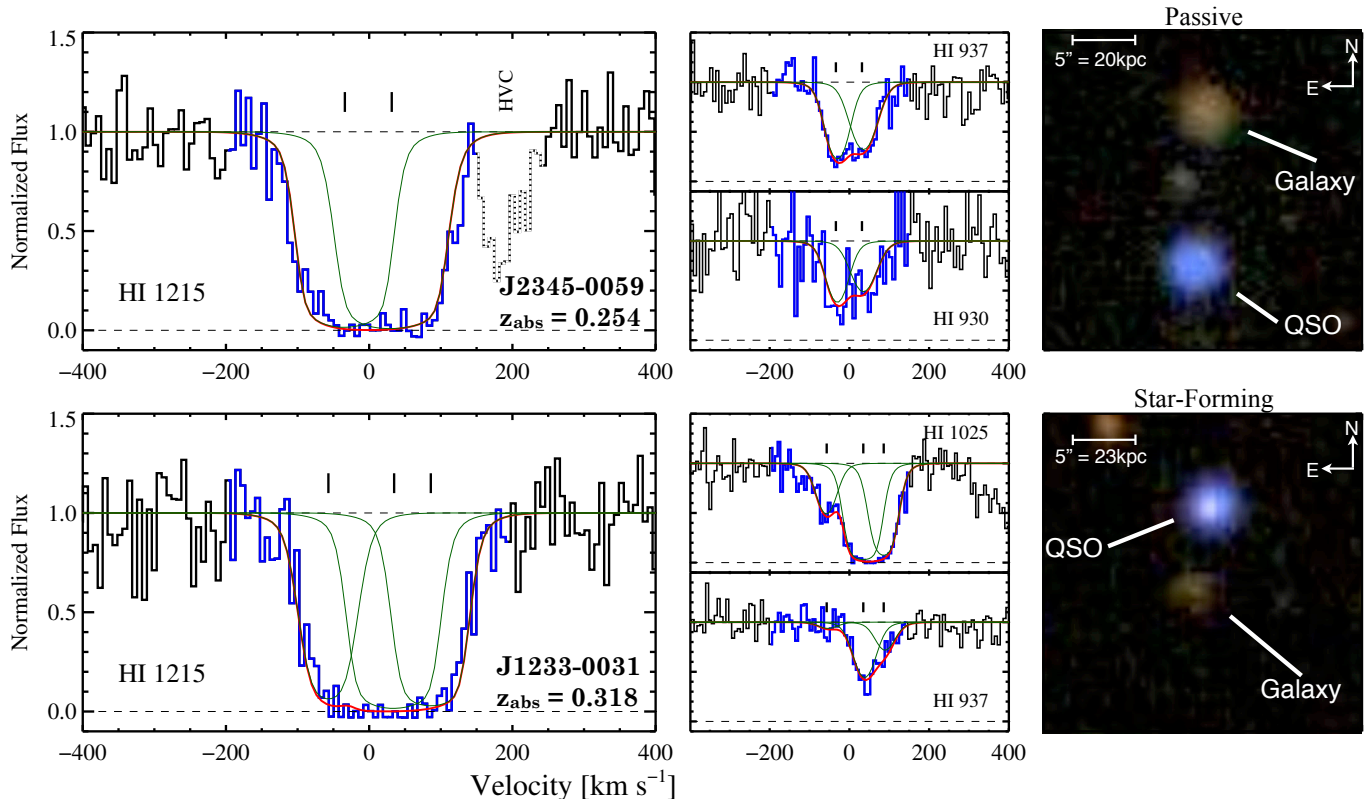


Figure 1. HI absorption profiles and SDSS images for two example passive (top) and star-forming (bottom) galaxies. The strong Ly α absorption profiles consist of multiple blended components, and are similar for both galaxies. Individual Voigt profile components are shown in green; composite profiles are in red. The weaker Lyman series lines in the middle panels constrain the component structure and intrinsic line widths, which in turn constrain the gas temperature (§ 5).

Most recently, Prochaska et al. (2011) found that strong Ly α absorption ($W_r > 300 \text{ m}\text{\AA}$) arises in galaxy halos—including less massive ETGs—within $\rho \simeq 300 \text{ kpc}$, but the majority of their pairs lie at large radii (only 3 pairs at $\rho < 200 \text{ kpc}$). Careful selection of QSO sightlines is therefore crucial to study the dependence of CGM gas within 150 kpc, and spectroscopy of the host galaxies is important to measure the current SFR and galaxy metallicities.

We designed the COS-Halos survey to probe the inner CGM of L^* galaxies at $z \sim 0.2$ and to test the prevailing theoretical picture of “hot” and “cold” accretion, which might be related to the observed star formation dichotomy in galaxies (Kereš et al. 2005; Dekel & Birnboim 2006). COS-Halos has several distinct advantages over previous work for assessing the amount and properties of CGM surrounding ETGs: (1) it systematically covers impact parameters 0 – 150 kpc and stellar masses $\log M_* = 10 - 11$ with galaxies from both color-magnitude sequences selected prior to knowledge of absorption, (2) the wavelength range of COS and the galaxy redshifts ($z \gtrsim 0.1$) generally allow for measurements of the weaker HI Lyman series lines that give better column densities and line broadening parameters than Ly α alone, and (3) the galaxies are well characterized by ground-based optical measurements of their stellar masses, SFRs, and metallicities. COS-Halos has previously found that highly ionized O VI in the halos

of ETGs occurs at much lower incidence than in star-forming galaxies, such that the presence of O VI out to $\sim 150 \text{ kpc}$ is related to star formation (Tumlinson et al. 2011b). We will present the full analysis of the HI absorption for our complete sample of 50 galaxies in a future paper (Tumlinson et al. 2012, in preparation). In this Letter, we present results for 16 ETGs from COS-Halos, showing that their associated HI gas is plentiful (§ 3), bound (§ 4), cold (§ 5), and may represent a large mass of baryons in their CGM (§ 6).

The COS-Halos survey obtained 39 spectra of QSOs at $z < 1$ with the Cosmic Origins Spectrograph (COS; Green et al. 2012) onboard the Hubble Space Telescope (HST) under program GO-11598 (PI Tumlinson). These data were reduced, co-added, and continuum-normalized with procedures outlined by Meiring et al. (2011), Tumlinson et al. (2011a), and Thom et al. (2011). We measured column densities for the absorption associated with targeted galaxies using both the apparent optical depth technique (AOD; Sembach & Savage 1992) and iterative Voigt profile fitting with the measured COS line spread function (Ghavamian et al. 2009). Our measurements for HI column density are weighted averages of unsaturated Lyman lines or profile fits to damped absorption. Where all available Lyman series lines are saturated we set a lower limit to N_{HI} with the highest-order detected Lyman line. The multi-component Voigt profile fitting yields N , b , and v for components within each system

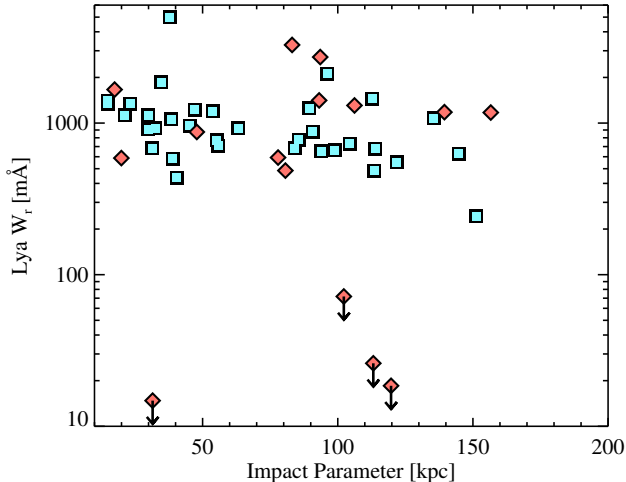


Figure 2. $\text{Ly}\alpha$ rest-frame equivalent width W_r versus impact parameter ρ for our COS-Halos sample of SF (blue) and ETG (red) galaxies. Note that only 15 ETGs appear in this figure, since in 1 case we do not have coverage of the $\text{Ly}\alpha$ transition. Even with four low values seen in the ETGs, there is no statistically significant evidence of a dependence on galaxy type (red vs. blue).

that are used in § 5.

The medium-resolution Keck and Magellan spectroscopy used to derive the properties of the galaxies in the sample (SFRs, metallicities, etc) are described fully by Werk et al. (2012). The resulting sample contains 16 galaxies classified as passive and/or early type, based on their lack of star-formation ($s\text{SFR} = \text{SFR}/M_* < 10^{-11} \text{ M}_\odot \text{ yr}^{-1}$, Werk et al. 2012). We caution that these fields have not been uniformly surveyed for all galaxies down to low luminosity limits to eliminate all other possible associations, but these observations empirically describe the distribution of gas around ETGs as a function of impact parameter, whatever its source. Figure 1 shows an example of an ETG and star-forming galaxy from our sample. The composite image from the Sloan Digital Sky Survey (SDSS) is shown, along with the $\text{Ly}\alpha$ absorption owing to the galaxy. Both galaxies have similar H I column densities and absorption profiles.

3. STRONG H I IS COMMON AROUND EARLY-TYPE GALAXIES

Figure 2 plots the $\text{Ly}\alpha$ rest-frame equivalent width W_r , as a function of impact parameter ρ , and shows the remarkable similarity in H I strength between the ETG (red) and SF (blue) samples. A KS test on W_r does not provide significant evidence against the null hypothesis that the two distributions are drawn from the same parent population ($D = 0.32$, $P = 0.19$). The four $\text{Ly}\alpha$ non-detections drive the difference in the KS statistic, and offer a hint that the distributions may be slightly different, but we cannot separate the distributions in a statistical fashion; a larger sample of ETGs will be needed to show if this difference is real.

We also calculated the “covering fraction” f_{hit} of H I detections. Even if we conservatively assume that the absorbers have the $N_{\text{H I}}$ given by the lower limits for saturated lines, we find that the covering fraction above $\log N_{\text{H I}} = 16$ is $f_{\text{hit}} = 0.21$ for SF galaxies, and $f_{\text{hit}} =$

0.38 for the ETGs. This column density has significance as the threshold above which Stewart et al. (2011) predicted essentially no absorbers surrounding halos at the ETG mass scale, owing to the transition between hot and cold accretion. Our covering fraction result rules out $f_{\text{hit}} = 0.01$ at $>99.9\%$ confidence. The corresponding covering fractions at $\log N_{\text{H I}} > 15$ are $f_{\text{hit}} = 0.64$ (SF) and $f_{\text{hit}} = 0.56$ (ETGs), again consistent to within the statistical errors of 0.15-0.2. Thus we find that strong H I absorption is common around the ETGs, and that to the limits of our survey, it does not appear significantly less often or weaker than in the halos of star-forming galaxies.

4. THE STRONG H I IS BOUND TO ITS HOST GALAXY

The detected H I shows a strong relationship to the targeted ETGs. It is found at separations consistent with being well inside the virial radius ($R_{\text{vir}} \sim 300 \text{ kpc}$), and it is closely associated with the stars in velocity space. Figure 3 shows the *full* velocity range of the detected H I absorption with respect to the systemic velocity of the galaxy’s stars (set to $v = 0$). The relative errors between absorption and galaxy redshift (i.e. between the wavelength solutions of the optical and COS spectroscopy) is $\sim 30 \text{ km s}^{-1}$. The filled symbols mark centroid velocities of the fitted components, while the range bars show the full width at zero absorption, a measure of the greatest kinematic extent of the detected H I. These velocities are plotted with respect to the inferred dark matter halo mass, which is derived from the photometrically-estimated stellar mass using the mean relation from Moster et al. (2010). The dashed curves show the escape velocity from the halos as a function of mass, at distances of 50, 100, and 150 kpc (from outside to inside). Nearly all the detected H I is found at velocities below the escape velocity. This is true even if we increase the velocity ranges by $\sqrt{3}$ to account for unconstrained projection effects (since relative Doppler shifts are a sightline-projected lower limit to the true 3D space motion). It is also possible that some of the detected ionized gas is in fact bound to satellite galaxies in the vicinity of the targeted galaxy¹⁰; if so, the kinematics suggest that the satellites are themselves bound and would be counted among the CGM mass budget for the host galaxy. We conclude that the detected H I is predominantly bound to its host galaxy, and not escaping at the time it is observed.

5. THE STRONG H I IS COLD COMPARED WITH HALO VIRIAL TEMPERATURES

Because COS-Halos typically covers multiple Lyman series lines at $z \gtrsim 0.2$ (Figure 1), we can often derive line-broadening parameters that are not available when relying solely on $\text{Ly}\alpha$ (which is almost always saturated). We perform profile fits to derive $N_{\text{H I}}$ and Doppler b for each component, where possible. These line widths provide robust upper limits on the gas temperature under the assumption that the broadening is purely thermal, $b \equiv \sqrt{2kT/m_H}$. From the measured Doppler parameters (Figure 4) we can firmly establish temperature upper limits of $T \lesssim 2 \times 10^5 \text{ K}$ ($b_{\text{therm}} < 60 \text{ km s}^{-1}$), with

¹⁰ This is very likely in the two systems with $\log N_{\text{H I}} > 10^{19}$.

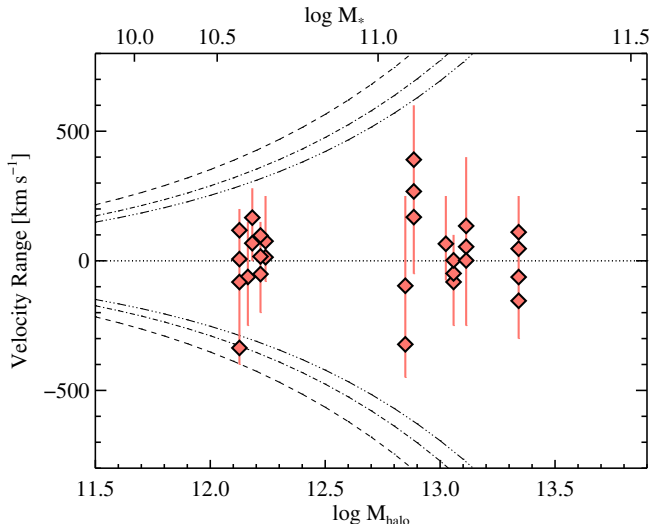


Figure 3. The full velocity range occupied by the detected HI absorption, with respect to the galaxy systemic redshift ($v = 0$), plotted versus the inferred dark-matter halo mass for our sample. The fitted component positions are indicated by the diamonds, while the full velocity ranges are shown by the vertical red bar. The three dashed lines mark the halo escape velocity at 50, 100, and 150 kpc, from outside to inside. All the HI detected in the ETGs is well inside the halo escape velocity, suggesting that is bound to the host galaxies.

80% at $T < 10^5$ K ($b_{\text{therm}} = 40$ km s $^{-1}$). These line widths are upper limits based on the observed profiles, and can only decrease if the observed profile turns out to be composed of narrower unresolved components, or is significantly affected by non-thermal broadening (which has shown to be common; Thom & Chen 2008; Tripp et al. 2008)¹¹.

We therefore conclude that the detected HI traces mainly “cool” (possibly photoionized) gas, at temperatures well below the $\gtrsim 10^6$ K virial temperatures of halos in this mass range. These temperatures resemble the expectations for the “cold mode” of galaxy gas accretion. Together with the finding that the detected gas is plentiful and bound, this finding suggests that the deposition of cold gas into galaxy halos (from the inside or the outside) and/or the formation of clouds at $\ll T_{\text{vir}}$ are not fully quenched even in galaxies that have ceased to form stars.

6. IMPLICATIONS FOR THE CGM MASS

The total mass of cool gas in ETG halos is of interest in comparison to their stellar masses and interstellar gas reservoirs. Having measured the covering fraction and typical column density, we can estimate the detected HI mass from physical arguments and simple models. The simplest possible mass estimate comes from multiplying a surface density by an area:

$$M_{\text{HI}} = \pi R^2 \langle N_{\text{HI}} \rangle m_{\text{H}} f_{\text{hit}} \\ \geq 2.8 \times 10^6 \left(\frac{N_{\text{HI}}}{10^{16}} \right) \left(\frac{f_{\text{hit}}}{0.5} \right) \left(\frac{R}{150 \text{ kpc}} \right)^2 M_{\odot}$$

¹¹ There may also be shallow “broad Lyman α ” (BLA) absorption hidden in the profiles; we cannot draw any conclusions about the presence or absence an additional hot gas component in ETGs.

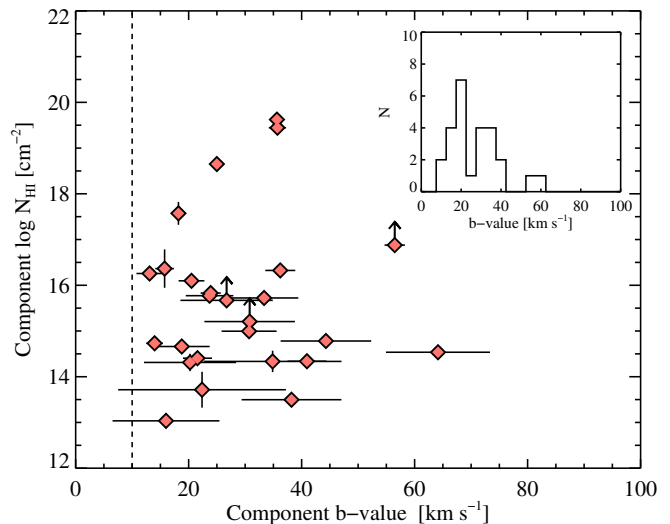


Figure 4. On a component-by-component basis, the N_{HI} and Doppler b parameter for HI around ETGs. Even if we assume that there are no non-thermal contributions to the line-broadening, most of the detected HI has implied temperatures of $T \lesssim 2 \times 10^5$ K.

where we have taken a typical $N_{\text{HI}} = 10^{16}$ cm $^{-2}$, at which the hit rate is $f_{\text{hit}} = 0.5$ for ETGs, and $\rho = 150$ kpc. This mass of HI is strictly a lower limit because we have taken the typical minimum N_{HI} permitted by the profiles of saturated lines and surveyed a radius that may not encompass the full CGM mass (c.f. Prochaska et al. 2011). The corresponding total mass of CGM hydrogen is $M_{\text{H}} = M_{\text{HI}}/f_{\text{HI}}$, where f_{HI} is the typical neutral fraction in the gas. Thus the ionization correction is the major factor in setting the total mass, but the ionization conditions, and thus the total mass of the CGM gas, depend on the unknown temperature and density of the detected material. Modestly overdense gas in the CGM should be exposed to the cosmic ionizing background radiation, which will further suppress the neutral fraction and imply a much larger mass.

To estimate what CGM masses are possible for the ETGs we show a simple halo model in Figure 5 that uses a power-law gas density profile exposed to a uniform ionizing background and held at fixed temperature. The gas density follows a power-law dependence with radius, $n \propto (R/R_{\text{vir}})^{-\alpha}$, with $\alpha = 2$, normalized to a specific cosmic overdensity δ_0 at R_{vir} . The photoionization equilibrium solutions were derived using Cloudy (Ferland et al. 1998) models and including ionization by the Haardt & Madau photoionizing background (for $z = 0.2$) and the temperature-dependent collisional ionization equilibrium (CIE). We neglect any photoionizing contribution from the nearby ETGs since their star-formation rates are not high enough to contribute significantly to the 1 Ryd background in their halos (Tumlinson et al. 2011a). Overdensities of $\delta_0 = 20 - 50$ are required to match the ETG HI detections with $\log N_{\text{HI}} \sim 16$. This profile gives a total mass of $\log M_{\text{H}} \sim 11$. The lower model adopts $\delta_0 = 2$, and is a better match to the non-detections. Note that the results depend less on the chosen temperature than on the density normalization. From these simple models we conclude that the detected CGM is consistent with a mass $M_{\text{CGM}} \gtrsim 10^{9-11} M_{\odot}$. This mass is significant

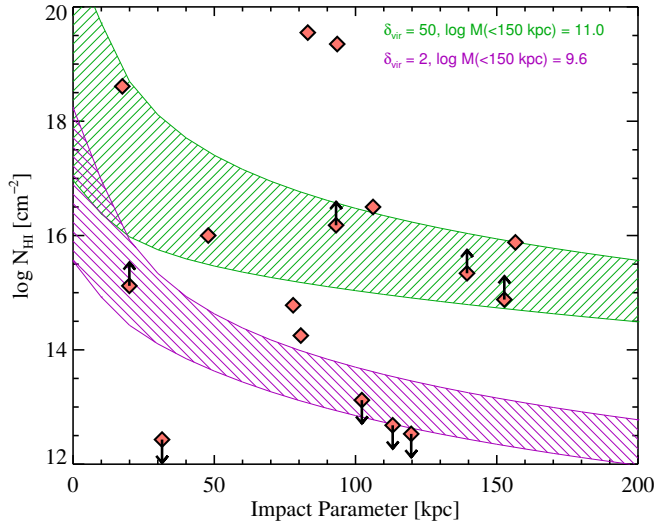


Figure 5. N_{HI} versus impact parameter ρ for all 16 ETGs. Lower limits are systems for which all available Lyman lines are saturated. The model profiles show two simple halo models for overdensity normalization $\delta_{\text{vir}} = 50$ (upper pair, green) and $\delta_{\text{vir}} = 2$ (lower pair, purple). Within each set of curves the lower curve corresponds to $T = 10^5$ K, while the upper bounding curves are for $T = 10^{4.3}$ K; these are the two relevant temperature limits from the kinematics analysis above. The total gas masses inside 150 kpc are $\log M(<150 \text{ kpc}) = 9.6 - 11$.

by comparison with the *interstellar* gas masses detected in other ETGs (§ 1). At the high end these masses are potentially significant reservoirs of “missing baryons” in the budgets of these massive halos. We emphasize that these simple models are not rigorous derivations of the ionization correction, from which the actual gas column densities N_H can be inferred. We will publish separately a full analysis of the gas column densities based on models calibrated to the many available metal lines in these absorbers (J. K. Werk et al. in preparation). Rather, these simple estimates show that ETGs harbor a significant mass of cold, bound gas in their CGM.

7. IMPLICATIONS

The COS-Halos survey has detected significant quantities of cool, likely photoionized gas bound to the halos of massive early-type galaxies. The cool gas does not appear to be correlated with star-formation, in stark contrast with O VI, which is strongly dependent on the presence or absence of star-formation (Tumlinson et al. 2011b). The cool gas reservoir may contribute $\gtrsim 10^9 - 10^{11} M_\odot$ of gas to the halos of ETGs, comparable to the interstellar reservoirs (§ 1), and exists at well below the halo virial temperatures. This material is typically well within the escape velocities of the host galaxies, so it may be re-accreted by the galaxies and eventually used for star-formation. The question then becomes, why does the gas not do so?

These ETGs have been quenched, in the usual sense that they are no longer forming stars. These strong H I absorbers and the cool CGM they trace were predicted to disappear at the end of cold accretion, which should not operate in halos at this mass (Stewart et al. 2011). If $M_{\text{CGM}} \sim 10^{10} M_\odot$ is typical of the star forming galaxies in COS-Halos as well as the ETGs, then the ETGs probably have less mass in their CGM *relative to their stellar*

and halo masses than the SF galaxies (at least in cool gas). This might be the signature of quenching that can suppress but not completely remove cold gas from the halo, or that the gas can reaccrete long after quenching. It is also possible that the quenching mechanism *did* remove all the CGM gas, after which cold clouds re-accrete from the IGM or reform from thermal instabilities in the hot corona.

Models that attempt to explain the formation and evolution of ETGs will need to account for this significant budget of cold gas in their halos. While it is possible that some of this gas is the direct product of ejection by supernovae while star-formation was occurring, it is perhaps more likely to be gas cooled from their hot halos or falling in from the IGM. In this case, preventive feedback may act to slow its accretion, allowing only small budgets of interstellar gas to enter the ISM and form stars. Some of it (especially the stronger systems) may be bound to satellites that are themselves bound to the host, and thus present or future contributors to the diffuse CGM. In any case, our findings indicate that the quiescence of star formation in ETGs generally cannot be attributed exclusively to the quenching of gas in their circumgalactic medium.

Support for program GO11598 was provided by NASA through a grant from the Space Telescope Science Institute, which is operated by the Association of Universities for Research in Astronomy, Inc., under NASA contract NAS 5-26555. Some of the data presented herein were obtained at the W.M. Keck Observatory, which is operated as a scientific partnership among the California Institute of Technology, the University of California and the National Aeronautics and Space Administration. TMT appreciates support from NASA grant NNX08AJ44G. MSP acknowledges support from the Southern California Center for Galaxy Evolution, a multi-campus research program funded by the University of California Office of Research.

REFERENCES

- Baldry, I. K., Glazebrook, K., Brinkmann, J., et al. 2004, *ApJ*, 600, 681
- Bell, E. F., Wolf, C., Meisenheimer, K., et al. 2004, *ApJ*, 608, 752
- Bland-Hawthorn, J., Sutherland, R., Agertz, O., & Moore, B. 2007, *ApJ*, 670, L109
- Chen, H., & Mulchaey, J. S. 2009, *ApJ*, 701, 1219
- Chen, H.-W., Lanzetta, K. M., Webb, J. K., & Barcons, X. 2001, *ApJ*, 559, 654
- Crocker, A. F., Bureau, M., Young, L. M., & Combes, F. 2011, *MNRAS*, 410, 1197
- Davis, T. A., Alatalo, K., Sarzi, M., et al. 2011, *MNRAS*, 417, 882
- Dekel, A., & Birnboim, Y. 2006, *MNRAS*, 368, 2
- Faber, S. M., Willmer, C. N. A., Wolf, C., et al. 2007, *ApJ*, 665, 265
- Ferland, G. J., Korista, K. T., Verner, D. A., et al. 1998, *The Publications of the Astronomical Society of the Pacific*, 110, 761
- Ghavamian, P., Aloisi, A., Lennon, D., et al. 2009, *Preliminary Characterization of the Post-Launch Line Spread Function of COS*, Tech. rep.
- González, J. J. 1993, PhD thesis, Thesis (PH.D.)—UNIVERSITY OF CALIFORNIA, SANTA CRUZ, 1993. Source: Dissertation Abstracts International, Volume: 54-05, Section: B, page: 2551.
- Green, J. C., Froning, C. S., Osterman, S., et al. 2012, *ApJ*, 744, 60
- Kaviraj, S. 2010, *MNRAS*, 408, 170

- Kereš, D., Katz, N., Weinberg, D. H., & Davé, R. 2005, *Monthly Notices of the Royal Astronomical Society*, 363, 2
- Lees, J. F., Knapp, G. R., Rupen, M. P., & Phillips, T. G. 1991, *ApJ*, 379, 177
- Meiring, J. D., Tripp, T. M., Prochaska, J. X., et al. 2011, *ApJ*, 732, 35
- Moster, B. P., Somerville, R. S., Maulbetsch, C., et al. 2010, *ApJ*, 710, 903
- Oosterloo, T., Morganti, R., Crocker, A., et al. 2010, *MNRAS*, 409, 500
- Prochaska, J. X., Weiner, B., Chen, H.-W., Mulchaey, J., & Cooksey, K. 2011, *ApJ*, 740, 91
- Putman, M. E., Saul, D. R., & Mets, E. 2011, *MNRAS*, 418, 1575
- Sembach, K. R., & Savage, B. D. 1992, *ApJS*, 83, 147
- Serra, P., Oosterloo, T., Morganti, R., et al. 2011, *ArXiv e-prints*
- Springel, V., Di Matteo, T., & Hernquist, L. 2005, *ApJ*, 620, L79
- Stewart, K. R., Kaufmann, T., Bullock, J. S., et al. 2011, *ApJ*, 735, L1
- Thom, C., & Chen, H.-W. 2008, *ApJS*, 179, 37
- Thom, C., Werk, J. K., Tumlinson, J., et al. 2011, *ApJ*, 736, 1
- Thomas, D., Maraston, C., Schawinski, K., Sarzi, M., & Silk, J. 2010, *MNRAS*, 404, 1775
- Tonnesen, S., & Bryan, G. L. 2009, *ApJ*, 694, 789
- Trager, S. C., Faber, S. M., Worthey, G., & González, J. J. 2000, *AJ*, 119, 1645
- Tripp, T. M., Sembach, K. R., Bowen, D. V., et al. 2008, *ApJS*, 177, 39
- Tumlinson, J., Werk, J. K., Thom, C., et al. 2011a, *ApJ*, 733, 111
- Tumlinson, J., Thom, C., Werk, J. K., et al. 2011b, *Science*, 334, 948
- Wakker, B. P., & Savage, B. D. 2009, *ApJS*, 182, 378
- Werk, J. K., Prochaska, J. X., Thom, C., et al. 2012, *ApJS*, 198, 3
- Young, L. M., Bureau, M., Davis, T. A., et al. 2011, *MNRAS*, 414, 940